Metabolome analysis of masseter muscle in senescence-accelerated mouse-prone 8 (SAMP8)

Yoshiaki Kato
Department of Oral Pathobiological Science and Surgery, Tokyo Dental College
Teruhide Hoshino (hoshinoteruhide@tdc.ac.jp)
Department of Oral Pathobiological Science and Surgery, Tokyo Dental College
Yudai Ogawa
Department of History and Developmental Biology, Tokyo Dental College
Keisuke Sugahara
Department of Oral Pathobiological Science and Surgery, Tokyo Dental College
Akira Katakura
Department of Oral Pathobiological Science and Surgery, Tokyo Dental College

Research Article

Keywords: masseter muscle, senescence-accelerated mouse-prone 8 (SAMP8), frailty

Posted Date: April 27th, 2021

DOI: https://doi.org/10.21203/rs.3.rs-389321/v1

Abstract

Frailty is a vulnerable state that marks the transition to long-term care for the elders. Recently, the relationship between frailty and oral function has been attracting attention. By clarifying the specific metabolic changes in the masseter muscle, we aimed to contribute to maintenance of masticatory function. The purpose of this study is to clarify the changes in masseter muscle of senescence-accelerated mouse-prone 8 (SAMP8) mice metabolites and metabolic pathways due to aging. Capillary electrophoresis-mass spectrometry metabolome analysis was performed on the masseter muscle of 12-week-old, 40-week-old, and 55-week-old mice. Expression analysis was performed by reverse transcription polymerase chain reaction (RT-PCR) and immunofluorescence for the metabolome pathways extracted by metabolome analysis that considered to be related to aging. Nineteen metabolites had a significant difference in absolute quantitative values and were considered to affect the first principal component by factor loading. The extracted metabolic pathways were glycolysis, polyamine metabolome pathway, and purine metabolome pathway. RT-PCR was performed on the extracted metabolome pathways. Expression of the spermidine synthase and hypoxanthine phosphoribosyl transferase genes with significant differences by RT-PCR was confirmed by immunofluorescence. The metabolic pathways considered to be related to aging in masseter muscle were glycolysis, polyamine metabolic pathway, and purine metabolic pathway.

Introduction

Frailty is a vulnerable state which marks the transition to long-term care for the elders and an increase in their risks of health problems, falls and death [1]. Sarcopenia is the main symptom of frailty. The early detection and prevention of sarcopenia is important to ensure an excellent quality of life for the aged.

Fundamental research on aging has been conducted with the use of aging animals. Leann et al. measured the cross-sectional area of the soleus muscle in Fischer 344 Brown Norway (FBNF1) rats and reported the atrophy of fast-twitch muscles and notable changes in old age [2]. Guo et al. observed morphological and immunohistochemical changes over time in the gastrocnemius muscle of senescence-accelerated mouse-prone 8 (SAMP8) mice and reported that sarcopenia appeared when they were 40 weeks old [3]. Furthermore, Uchitomi et al. performed metabolome analysis on the gastrocnemius muscle of aged C57BL/6J mice to search for metabolites that fluctuate due to aging [4]. Consequently, they reported a decrease in glucose metabolites, a decrease in polyamine metabolites, and an increase in neurotransmitters.

Recently, the relationship between frailty and oral function has been attracting attention in the subject of numerous studies. For instance, in an epidemiological study, Murakami et al. conducted a survey of community-dwelling older people in Japan and reported that sarcopenia was associated with the masticatory function [5]. Meanwhile, Iwasaki et al. reported that maximum bite force was associated with frailty [6]. Moreover, the concept of oral frailty was proposed for the early detection of slight deterioration in the aged, and the characteristic of poor diadochokinesis, constitutes the first step toward oral

disfunction. Oral frailty is also associated with the prognosis of curtailed longevity [7]. We have noted that there are only a few defining studies that relate the deterioration of oral health to aging. Hoshino et al. reported that the atrophy of the masseter muscle in SAMP8 mice had occurred by the time they were 40 weeks old and that there were subsequent changes in muscle contraction characteristics [8]. However, there are no reports of the molecular biological examination of the masseter muscle during aging. Given this context, we focused on the metabolites in this study. By clarifying the specific metabolic changes in the masseter muscle, we aimed to contribute to maintenance of masticatory function. Hence, the purpose of this study is to clarify the changes in masseter muscle metabolites and metabolic pathways due to aging. We verified the results through a metabolome analysis of the masseter muscles of SAMP8 mice [8], as the changes due to aging have already been confirmed, in this type of young mice (12-week-old), elderly mice (40-week-old), and later stage elderly mice (55-week-old).

Results

Body weight

The mean body weight of the mice was 28.9 ±1.01 g at 12 weeks old, 39.22 ±3.43 g at 40 weeks old, and 39.96±3.79 g at 55 weeks old (Fig. 1a). While body weight increased between weeks 12 and 40, and between weeks 12 and 55, there was no difference in weight between 40-week-old and 55-week-old mice.

Amount of food intake

The mean weekly food intake was 36.2±3.88 g at 12 weeks old, 39.8±6.01 g at 40 weeks old, and 25.6±0.76 g at 55 weeks old (Fig. 1b). Food intake decreased between 12 weeks and 55 weeks, and between 40 weeks and 55 weeks, whereas there was no difference in food consumption between 12-week-old and 40-week-old mice.

Metabolome analysis (masseter muscle)

A principal component analysis (PCA) demonstrated that the metabolites contributing to the first principal component could be clearly distinguished at each age (Fig. 2a). Hierarchical cluster analysis (HCA) also revealed changes in metabolite profiles (Fig. 2b). Moreover, clear metabolic fluctuations were observed from 40 weeks to 55 weeks.

Metabolites that fluctuated between 40 weeks and 55 weeks

There were significant differences in the absolute quantitative values of 36 substances (Table. 1), 20 of which were elevated metabolites and 16 were lowered metabolites. Furthermore, the factor loadings that affected the first principal component were 10 elevated substances and 9 lowered substances (Table 2). Moreover, significant changes were observed in the polyamine metabolic pathway, purine metabolic pathway, and glycolysis pathway.

Since the polyamine metabolic pathway is associated with cell proliferation, protein synthesis, and nucleic acid synthesis, a significant increase in S-adenosylmethionine and spermidine was observed (Fig. 3).

Since the purine metabolic pathway is related to purine nucleotide metabolism and ATP resynthesis, a significant increase in IMP, GMP, GDP, and hypoxanthine, and a significant decrease in GTP and ATP were observed (Fig. 4).

We observed a decrease in 3-phosphoglyceric acid, 2-phosphoglyceric acid, and phosphoenolpyruvic acid, which are engaged in glycolysis (Fig. 5).

Additionally, we observed an increase in the neurotransmitter choline and a decrease in phosphocreatine, which is used for ATP synthesis and to produce creatinine, which is a reaction product.

Reverse transcription polymerase chain reaction (RT-PCR)

We confirmed the expression of enzymes that are involved in the polyamine and purine metabolic pathways and that fluctuated between 40-week-old and 55-week-old mice. In the polyamine metabolic pathway, we observed a significant increase in the expression of the spermidine synthase gene (SRM) in 55-week-old mice compared with 40-week-old mice ($p = 0.002$) (Fig. 6 a). Furthermore, we observed a significant increase in the expression of the hypoxanthine phosphoribosyl transferase gene (HPRT), an enzyme used in the salvage circuit of ATP resynthesis ($p = 0.048$) in the purine metabolic pathway (Fig. 6 b).

Immunohistochemical observations

The SRM of the polyamine metabolic pathway was expressed surrounding the muscle fibers, especially in the interstitium (Fig. 7). The HPRT of the purine metabolic pathway was also expressed surrounding the muscle fibers. (Fig. 8).

Discussion

The body weight of SAMP8 mice is said to increase between the age of 8 weeks and 24 weeks [9]. Similarly, in this study, the body weight tended to increase as the mice aged. Furthermore, there was no clear individual difference during the raising stage. Moreover, aging physiologically reduces food intake, and anorexia due to aging leads to energy malnutrition and weight loss [10]. We observed a decrease in food intake between 12-week-old and 55-week-old mice, and between 40-week-old and 55-week-old mice. However, since it is not accompanied by weight loss, it can be inferred that it was not a case of simple undernutrition. Consequently, to clarify the relationship between body weights and food intakes, we considered that other factors such as lean body mass and whole-body muscle mass should be measured. We also considered that nutritional indicators such as blood cholesterol level and blood hemoglobin should be examined.

The masseter muscle consists of predominantly fast-twitch muscle, with many MyHC Type II fibers distributed among the muscle fibers. Fast-twitch muscle fibers have high enzymatic activity and creatine kinase activity that compose glycolysis and have excellent anaerobic metabolic capacity [11]. Studies indicate that glycolytic metabolites of skeletal muscle decrease with aging [4]. In the gastrocnemius muscle, fructose 1,6-diphosphate, dihydroxyacetone phosphate, and glyceraldehyde 3-phosphate (upstream metabolites) decreased [4]. Our results indicated a decrease in glycolytic metabolites. These metabolites were 3-phosphoglyceric acid, 2-phosphoglyceric acid, and phosphoenolpyruvic acid (downstream metabolites). MyHC Type IIb fibers decrease in the masseter muscle of SAMP8 mice, notably between 40-week-old and 55-week-old mice [8], which decline could be associated with the aforementioned decrease. The dephosphorylation of 1,3-bisphosphoglyceric acid produces 3-phosphoglyceric acid. This reaction is accompanied by ATP production through the phosphorylation of ADP. Phosphoenolpyruvic acid is produced by the dehydration of 2-phosphoglyceric acid. This reaction is considered to produce pyruvic acid simultaneously to ATP by the transfer of a phosphate group to ADP. We suggest that the decrease in 3-phosphoglyceric acid, 2-phosphoglyceric acid, and phosphoenolpyruvic acid in the masseter muscle was caused by the consumption of a large amount of ATP required for masticatory movements.

Spermidine is an autophagy-related autoinducer [12]. Its concentration has been reported to decrease with age [13]. Moreover, its concentration decreases significantly in the gastrocnemius muscle of C57/BL6J mice [4]. In this study, we observed a significant increase of spermidine in the masseter muscle. Furthermore, in the masseter muscle, the expression of SRM, a gene for spermidine synthase, was confirmed in the interstitium by fluorescent immunohistochemical staining, and the expression was enhanced in the comparison between 40-week-old and 55-week-old mice. The same result was achieved by reverse transcription polymerase chain reaction (RT-PCR), and we believe that it participates in the synthesis of spermidine in the polyamine metabolic pathway. The masseter muscle's involvement in the masticatory function is essential to maintain a normal life. Additionally, there are reports that state autophagy is activated in comparison to the hind limbs, [14] and that masseter muscles in the young and elderly have similar performance to that of rats [15]. Based on these findings, we think that the masseter muscle, which is used more frequently than the hind limbs, is more susceptible to fatigue and aging, and a compensatory increase in spermidine induces autophagy activation, which might be correlated with maintaining functioning. As spermine is necessary for spermidine resynthesis [16], although no significant difference was observed in this research, it is considered that it decreases ($p = 0$) at 40 weeks due to the increase of spermidine at 55 weeks.

Furthermore, S-adenosylmethionine is involved in DNA methylation and is reported to increase with aging [17-19]. DNA methylation is a sign of slight changes in tissue composition such as tissue inflammation and fibrosis [20], and has become the subject of several studies as an epigenic biomarker of aging [21,22]. In this study, we confirmed that SAMP8 increased from 40-week-old to 55-week-old mice. We consider that this may decrease Type II fibers of the masseter muscle and the fluctuation in the polyamine metabolic pathway.

The purine metabolic pathway is engaged in ATP resynthesis during movement. Phosphocreatine is required for ATP synthesis [23], and hypoxanthine and IMP increases with movement [24]. According to the results, changes in glucose metabolism and the increase in hypoxanthine and IMP are maintained by the masticatory function in SAMP8's masseter muscle. We consider that the increased demand for energy sources ATP and GTP that leads to the activation of the salvage circuit for resynthesis may have caused the increase in HPRT. Furthermore, ATP was one of the factors responsible for the decrease in phosphocreatine. The expression of HPRT was confirmed by fluorescent immunohistochemical staining and RT-PCR, thus suggesting the activation of the salvage circuit of the purine metabolic pathway.

A limitation of this study is that aging changes in SAMP8 mice may differ from those in normal human aging. Although SAMP8 mice have a shorter lifespan than aged animals [25], and develop sarcopenia phenotype [3], we expect that they will be used in future studies on aging. In our study, SAMP8 mice were used to understand the characteristics of aging in the masseter muscle. Moreover, since humans and mice have different masticatory forms and muscle fiber composition, it may be unlikely that the results on mice will reflect the same changes that occur in humans.

However, these results will lead to the establishment of a masseter aging mechanism. Additionally, SAMR1 is often used as a control group for SAM. It has been previously confirmed that the masseter muscle in SAMP8 mice had histological changes due to aging when compared to SAMR1 mice [8]. Moreover, to further clarify the phenotype of the masseter muscle with aging, there is a need to compare it with the younger mice as in previous studies [4].

In conclusion, our results suggest that the age-related metabolic pathways of the masseter muscle on SAMP8 are likely to be the glycolysis and polyamine metabolome pathway and the purine metabolome pathway.

Methods

Animal experiment

SAMP8 mice were used in this study. SAMP8 is a type of mouse whose age accelerates between 16 weeks and 20 weeks, and is often used in aging research. The mice were raised for each of the following groups: 12-week-old (young) (N=4) to a stage before the start of accelerated aging; 40-week-old (elderly) (N=4) in the mean lifespan of SAMP8; 55-week-old (late elderly) (N=5) to a stage that exceeded the mean lifespan. In this study, the same species and the same age as those used in the previous studies [8] were used. The mice were raised in a 125×213×125 mm aluminum cage and were freely given food (Lab MR-A1) and water. Upon administering general anesthesia with isoflurane, the mice were euthanized by dislocating the cervical spines, and the masseter muscles were extracted. The experiments were conducted in accordance with the National Institutes of Health guidelines for care and use of animals and also approved by the Tokyo Dental College Institutional Animal Care and Use Committee (approval number: 202601). The study was carried out in compliance with the ARRIVE guidelines.

Body weight and the amount of food intake

In this study, body weight was measured once a week with an electronic scale (AND EW-1500i) and the food was weighed concurrently with a balance from 12-week-old to 55-week-old. The following week, the feed was again measured concomitantly with the mice's bodyweight, and the difference in the mass of the food between the two weeks represented the amount of food intake.

Capillary electrophoresis-mass spectrometry (CE-MS) metabolome analysis

Approximately 50 mg of frozen tissue was plunged into 750 μL of 50% acetonitrile/Milli-Q water containing internal standards (H33041002, Human Metabolome Technologies, Inc., Tsuruoka, Japan) at 0 °C to inactivate enzymes. The tissue was homogenized three times at 1,500 rpm for 2 min using a tissue homogenizer (Micro Smash MS100R, Tomy Digital Biology Co., Ltd., Tokyo, Japan) and then the homogenate was centrifuged at 2,300 ×g and 4 °C for 5 min. Subsequently, 400 μL of the upper aqueous layer was centrifugally filtered through a Millipore 5-kDa cutoff filter at 9,100 ×g at 4 °C for 120 min to remove proteins. The filtrate was centrifugally concentrated and re-suspended in 50 μL of Milli-Q water for capillary electrophoresis-mass spectrometry (CE-MS) analysis.

The metabolome analysis was performed with capillary electrophoresis time-of-flight mass spectrometry (CE-TOFMS) for cation analysis and CE-tandem mass spectrometry (CE-MS/MS) for anion analysis based on the methods described previously. This analysis focused on 116 central metabolites. CE-TOFMS analysis was conducted using an Agilent CE capillary electrophoresis system equipped with an Agilent 6210 time-of-flight mass spectrometer (Agilent Technologies, Waldbronn, Germany).

Quantitative analysis of expression metabolites

Total RNA extraction of the masseter muscle was performed using the RNeasy Mini Kit (Qiagen, Hilden, Germany) and Proteinase K (Takara Bio, Shiga, Japan). The cDNA was prepared using the QuantiTect Reverse Transcription Kit (Thermo Fisher Scientific, Waltham, MA, USA). The Double Delta Ct Value (ΔΔCt) method was used for quantification, and the relative expression level was compared to the expression of housekeeping genes in each sample.

For gene expression analysis, the TaqMan® gene expression assays (Thermo Fisher Scientific, Massachusetts, USA) were used in the RT-PCR 7500 realtime polymerase chain reaction (PCR) system (Thermo Fisher Scientific). This study focused on the polyamine and purine metabolic pathways, which were the most common metabolites that fluctuated between 40-week-old and 55-week-old mice. For target genes in the polyamine metabolic pathway, TaqMan® probes

(Thermo Fisher Scientific) used Methionine Adenosyl Transferase 2A (Mat2a) (Mm00728688_s1), SRM (Mm00726089_s1), spermine synthase (SMS) (Mm00786246_s1), Ornithine decarboxylase1 (Odc1) (Mm02019269_g1), spermine oxidase (Smox) (Mm01275475_m1), and S-adenosylmethionine decarboxylase (Amd2) (Mm04207265_gH). Meanwhile, in the purine metabolic pathway, TaqMan® probes used HPRT (Mm03024075_m1), phosphoribosyl pyrophosphate 1 (Prps1) (Mm00727494_s1),

adenine phosphoribosyl transferase (Mm04207855_g1), and xanthine dehydrogenase (Xdh) (Mm0044). In addition, the housekeeping gene β-actin (Mm00607939_s1) was used.

Immunohistochemical observations

The gathered masseter muscle was cut approximately 5 mm at the center of the belly of the muscle and fixed to a cork plate perpendicular to the muscle fibers. The specimens were rapidly frozen using isopentane cooled in liquid nitrogen. Frozen sections with a thickness of 4.5 μm and 20 μm were prepared using a cryostat M1950 (Leica, Nussloch, Germany), and then dried at room temperature for 60 min. In the immunohistochemical staining, the local expression of SRM in the polyamine metabolic pathway and HPRT in the purine metabolic pathway, which showed significant differences in gene expression, were observed in muscle fibers. The sections used for the SRM antibody were fixed with acetone for 10 min, and the sections used for the HPRT antibody were fixed with methanol for 10 min. After washing with PBS solution for 15 min, blocking was performed with 10% goat serum for 1 h and washed with PBS solution for 15 min. The primary antibody used was a 200fold diluted HPRT antibody (GeneTex, California, US) and SRM antibody (Proteintech, Chicago, US), and the specimen was incubated overnight at 4 °C after applying the primary antibody.

Furthermore, the secondary antibody, a goat anti-rabbit IgG antibody Alexa Fluor Plus 488 (Invitrogen, Massachusetts, US) was diluted 200-fold for the HPRT antibody and SRM antibody. To confirm the cytoskeleton, after applying the Acti-stain ™ 555 Fluorescent Phalloidin (Cytoskeleton Inc., Denver, US) secondary antibody, the sections were incubated at room temperature for 1 h under a shade. A universal microscope (Axioplan2 and Axiophot2, Carl Zeiss, Inc., Jena, Germany) and a confocal laser scanning microscope (LSM 880 with Airyscan, Carl Zeiss, Inc., Jena, Germany) were used for observation.

Statistical analyses

Statistical analyses were performed with IBM SPSS Statistics version 26 (IBM, Armonk, NY, USA) software. Moreover, for the statistics of body weight and food intake, Tukey's test was performed for the multiple comparison test. The metabolites, RT-PCR, and immunohistochemical stained areas of 40-week-old and 55-week-old mice were compared using Welch's t-test. The significance threshold was set at 5% ($p < 0.05$). The detection limit was described ($p=0$).

Declarations

Acknowledgement

We are sincerely grateful to Professor Sadamitsu Hashimoto, Department of Biology at Tokyo Dental College, who graciously provided guidance for the implementation of immunofluorescence.

Authors' Contributions

Y. K. and T. H. performed mouse experiment and collected the data. Y. K. and T. H., K.S. analyzed the data and undertook the statistical analyses. Y. O. performed immune histochemical analysis. Y.K. and T.H., A.K. prepared the manuscript and figure1-8,table1-2. All authors reviewed the results and approved the final version of the manuscript.

References

1. Fried, L. P., et al. Frailty in older adults: evidence for a phenotype. *J. Gerontol. A Biol. Sci. Med. Sci.* **56**(3)**,** M146-M156 (2001). 10.1093/gerona/56.3.m146, Pubmed:11253156
2. Leann, M. S., Linda, K. M. & Ladora, V. T. Adult and developmental myosin heavy chain isoforms in soleus muscle of aging Fischer Brown Norway rat. *Anat. Rec. A Discov Mol Cell Evol Biol.* **286A,** 866-873 (2005)
3. Guo, A. Y., et al. Muscle mass, structural and functional investigations of senescence-accelerated mouse P8 (SAMP8). *Exp. Anim.* **64**(4)**,** 425-433(2015). 10.1538/expanim.15-0025, Pubmed:26193895
4. Uchitomi, R., et al. Metabolomic analysis of skeletal muscle in aged mice. *Sci. Rep.* **9**(1)**,** 10425 (2019). 10.1038/s41598-019-46929-8, Pubmed:31320689
5. Murakami, M., et al. Relationship between chewing ability and sarcopenia in Japanese community-dwelling older adults. *Geriatr. Gerontol. Int.* **15**(8)**,** 1007-1012 (2015). 10.1111/ggi.12399, Pubmed:25363233
6. Iwasaki, M., et al. A 5-year longitudinal study of association of maximum bite force with development of frailty in community-dwelling older adults. *J. Oral Rehabil.* **45**(1)**,** 17-24 (2018). 10.1111/joor.12578, Pubmed:28965370
7. Tanaka, T. et al. Oral frailty as a risk factor for physical frailty and mortality in community-dwelling elderly. *J. Gerontol. A Biol Med. Sci.* **73**(12)**,** 1661-1667(2018). 10.1093/gerona/glx225, Pubmed:29161342
8. Hoshino, T., Yamamoto, M., Kasahara, K. & Katakura, A. Comparison of age-related morphological changes in the masseter muscles of senescence-accelerated mouse (SAM). *JOMSMP* **30**(1)**,** 44-49 (2018). 10.1016/j.ajoms.2017.07.006
9. Onishi, S., et al. Green tea extracts ameliorate high-fat diet– induced muscle atrophy in senescence-accelerated mouse prone-8 mice. *PLOS ONE* **13**(4)**,** e0195753 (2018). 10.1371/journal.pone.0195753, Pubmed:29630667
10. John, E. M. Decreased food intake with aging. *J. Gerontol. A Biol. Sci. Med. Sci.* **56a,** 81-88 (2001)
11. Yamashita, K. & Yoshioka, T. Profiles of creatine kinase isoenzyme compositions in single muscle fibres of different types. *J. Muscle Res. Cell Motil.* **12**(1)**,** 37-44 (1991). 10.1007/BF01781172, Pubmed:2050810
12. Pietrocola, F., et al. Spermidine induces autophagy by inhibiting the acetyltransferase EP300. *Cell Death Differ.* **22**(3)**,** 509–516 (2015). 10.1038/cdd.2014.215, Pubmed:25526088

13. Madeo, F., Bauer, M. A., Carmona-Gutierrez, D. & Kroemer, G. Spermidine: a physiological autophagy inducer acting as an antiaging vitamin in humans? *Autophagy* **15**(1), 165-168 (2019). 10.1080/15548627.2018.1530929, Pubmed:30306826
14. Iida, R. H., Kanko, S., Suga, T., Morito, M. & Yamane, A. Autophagic-lysosomal pathway functions in the masseter and tongue muscles in the klotho mouse, a mouse model for aging. *Mol. Cell. Biochem.* **348**(1–2), 89-98 (2011). 10.1007/s11010-010-0642-z, Pubmed:21082218
15. Norton, M., Verstegeden, A., Maxwell, L. C. & McCarter, R. M. Constancy of masseter muscle structure and function with age in F344 rats. *Arch. Oral Biol.* **46**(2), 139-146 (2001). 10.1016/s0003-9969(00)00107-2, Pubmed:11163321
16. Pegg, A. E. The function of spermine. *IUBMB Life* **66**(1), 8-18 (2014). 10.1002/iub.1237, Pubmed:24395705
17. Obata, F. & Miura, M. Enhancing S-adenosyl-methionine catabolism extends Drosophila lifespan. *Nat. Commun.* **6,** 8332 (2015). 10.1038/ncomms9332, Pubmed:26383889
18. Zykovich, A. et al. Genome-wide DNA methylation changes with age in disease-free human skeletal muscle. *Aging Cell* **13**(2), 360-366 (2014). 10.1111/acel.12180, Pubmed:24304487
19. Jin, C. J. et al. S-adenosyl-L-methionine increases skeletal muscle mitochondrial DNA density and whole body insulin sensitivity in OLETF rats. *J. Nutr.* **137**(2), 339-344 (2007). 10.1093/jn/137.2.339, Pubmed:17237308
20. Day, K. et al. Differential DNA methylation with age displays both common and dynamic features across human tissues that are influenced by CpG landscape. *Genome Biol.* **14**(9), R102 (2013). 10.1186/gb-2013-14-9-r102, Pubmed:24034465
21. Goel, N., Karir, P. & Garg, V. K. Role of DNA methylation in human age prediction. *Mech. Ageing Dev.* **166,** 33-41 (2017). 10.1016/j.mad.2017.08.012, Pubmed:28844970
22. Li, M. et al. DNA methylome: unveiling your biological age. *Protein Cell* **4**(10), 723-725 (2013). 10.1007/s13238-013-3913-0, Pubmed:24104390
23. Guimarães-Ferreira, L. Role of the phosphocreatine system on energetic homeostasis in skeletal and cardiac muscles. *Einstein* **12**(1), 126-131(2014). 10.1590/s1679-45082014rb2741, Pubmed:24728259
24. Jacek, Z. & Krzystof, K. Pathways of purine metabolism: effects of exercise and training in competitive athletes. *Trends Sport Sci.* **3**(22), 103-112 (2015)
25. Derave, W., Eijnde, B. O., Ramaekers, M. & Hespel, P. Soleus muscles of SAMP8 mice provide an accelerated model of skeletal muscle senescence. *Exp. Gerontol.* **40**(7), 562-572 (2005). 10.1016/j.exger.2005.05.005, Pubmed:16023814

Tables

Table. 1 List of significant changes in metabolites between 40-week-old and 55-week-old by absolute quantitative value. 55-week-old / 40-week-old.

No.	Compound name	Ratio	*p*-value	
1	γ-Aminobutyric acid	14	0.032	*
2	Adenylosuccinic acid	11	0.001	**
3	AMP	8.9	0.017	*
4	GMP	6.6	0.005	**
5	Argininosuccinic acid	5.2	0.003	**
6	Choline	4.6	0.002	**
7	IMP	3.8	3.9E-04	***
8	Spermidine	3.5	0.042	*
9	Galactose 1-phosphate	3.4	0.044	*
10	Hypoxanthine	2.9	0.027	*
11	Ribose 1-phosphate	2.7	0.008	**
12	Ribulose 5-phosphate	2.6	0.006	**
13	GDP	2.2	0.027	*
14	*S*-Adenosylhomocysteine	2.1	9.7E-05	***
15	2-Hydroxyglutaric acid	1.9	0.041	*
16	NADPH	1.7	4.1E-04	***
17	Pyruvic acid	1.5	0.008	**
18	*S*-Adenosylmethionine	1.4	0.004	**
19	Lactic acid	1.4	0.010	**
20	Val	1.3	0.027	*
21	*N*-Carbamoylaspartic acid	0.8	0.049	*
22	Gly	0.8	0.028	*
23	Urea	0.8	0.040	*
24	Hydroxyproline	0.8	0.007	**
25	$NADP^+$	0.7	0.012	*
26	Creatinine	0.7	0.008	**
27	Succinic acid	0.7	0.043	*
28	UDP-glucose	0.6	0.002	**
29	Malonyl CoA	0.5	0.009	**
30	NAD^+	0.5	2.7E-05	***
31	GTP	0.4	4.7E-04	***
32	ATP	0.3	5.0E-04	***
33	2-Phosphoglyceric acid	0.3	2.6E-04	***
34	3-Phosphoglyceric acid	0.3	1.0E-04	***
35	Phosphoenolpyruvic acid	0.2	0.004	**
36	Phosphocreatine	0.07	3.4E-04	***

“Ratio” is the comparative value of the relative areas (40-week-old vs. 55-week-old). The p-value was calculated using Welch’s *t*-test (***$p < 0.001$, **$p < 0.01$, *$p < 0.05$).

Table. 2 List of significant changes in metabolites between 40-week-old and 55-week-old by absolute quantitative value and factor loading. 55-week-old / 40-week-old.

No.	Compound name	Ratio	p-value	
1	Adenylosuccinic acid	11	0.001	**
2	GMP	6.6	0.005	**
3	Choline	4.6	0.002	**
4	IMP	3.8	3.90E-04	***
5	Spermidine	3.5	0.042	*
6	Hypoxanthine	2.9	0.027	*
7	Ribose 1-phosphate	2.7	0.008	**
8	GDP	2.2	0.027	*
9	S-Adenosylhomocysteine	2.1	9.70E-05	***
10	S-Adenosylmethionine	1.4	0.0041	**
11	Creatinine	0.7	0.008	**
12	NAD+	0.5	2.70E-05	***
13	Malonyl CoA	0.5	0.009	**
14	GTP	0.4	4.70E-04	***
15	3-Phosphoglyceric acid	0.3	1.00E-04	***
16	2-Phosphoglyceric acid	0.3	2.60E-04	***
17	ATP	0.3	5.00E-04	***
18	Phosphoenolpyruvic acid	0.2	0.004	**
19	Phosphocreatine	0.07	3.40E-04	***

(Glycolysis pathway : green, polyamine pathway : blue, purine pathway : red)

Figures

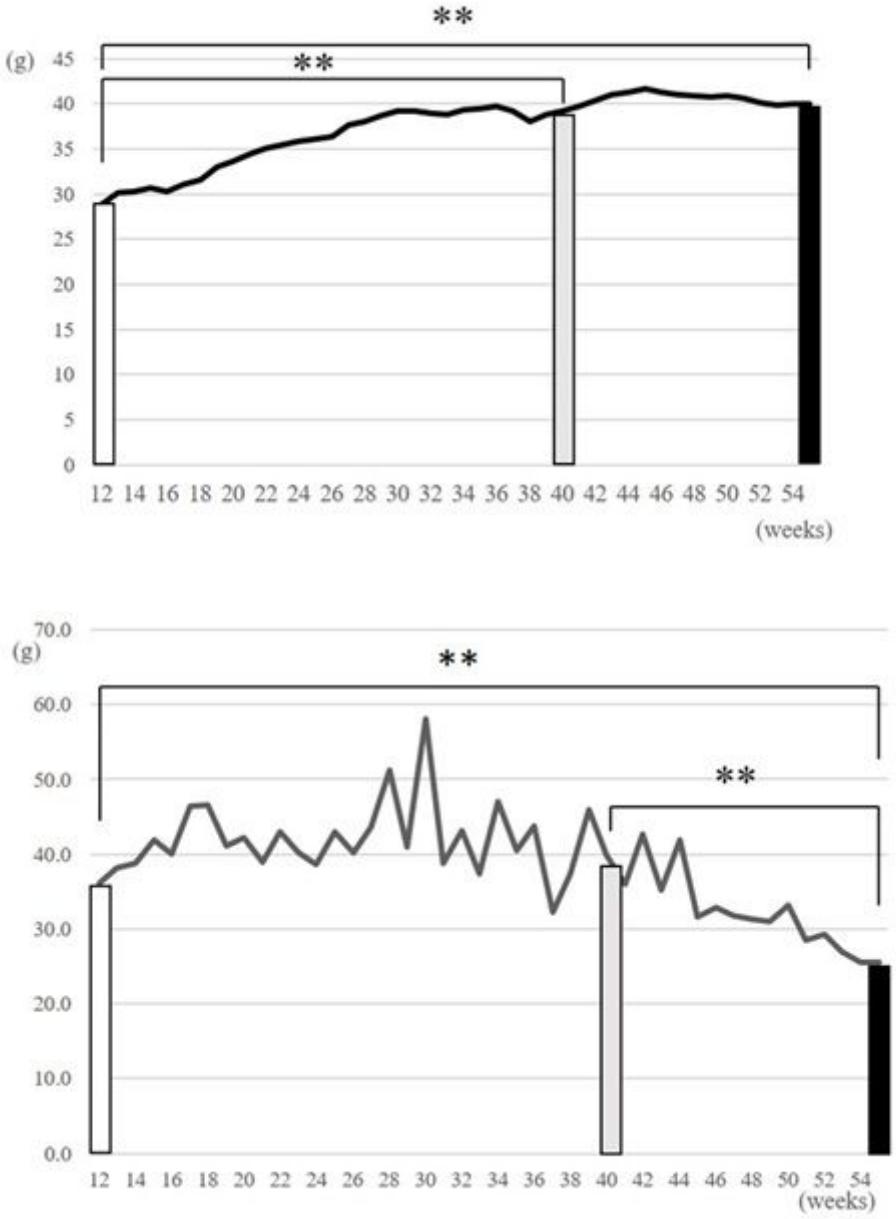

Figure 1

a Body weight Changes in body weights from 12-week-old to 55-week-old in five mice of 55-week-old. Body weights was measured weekly. (** $p < 0.01$). b Amount of feed intake

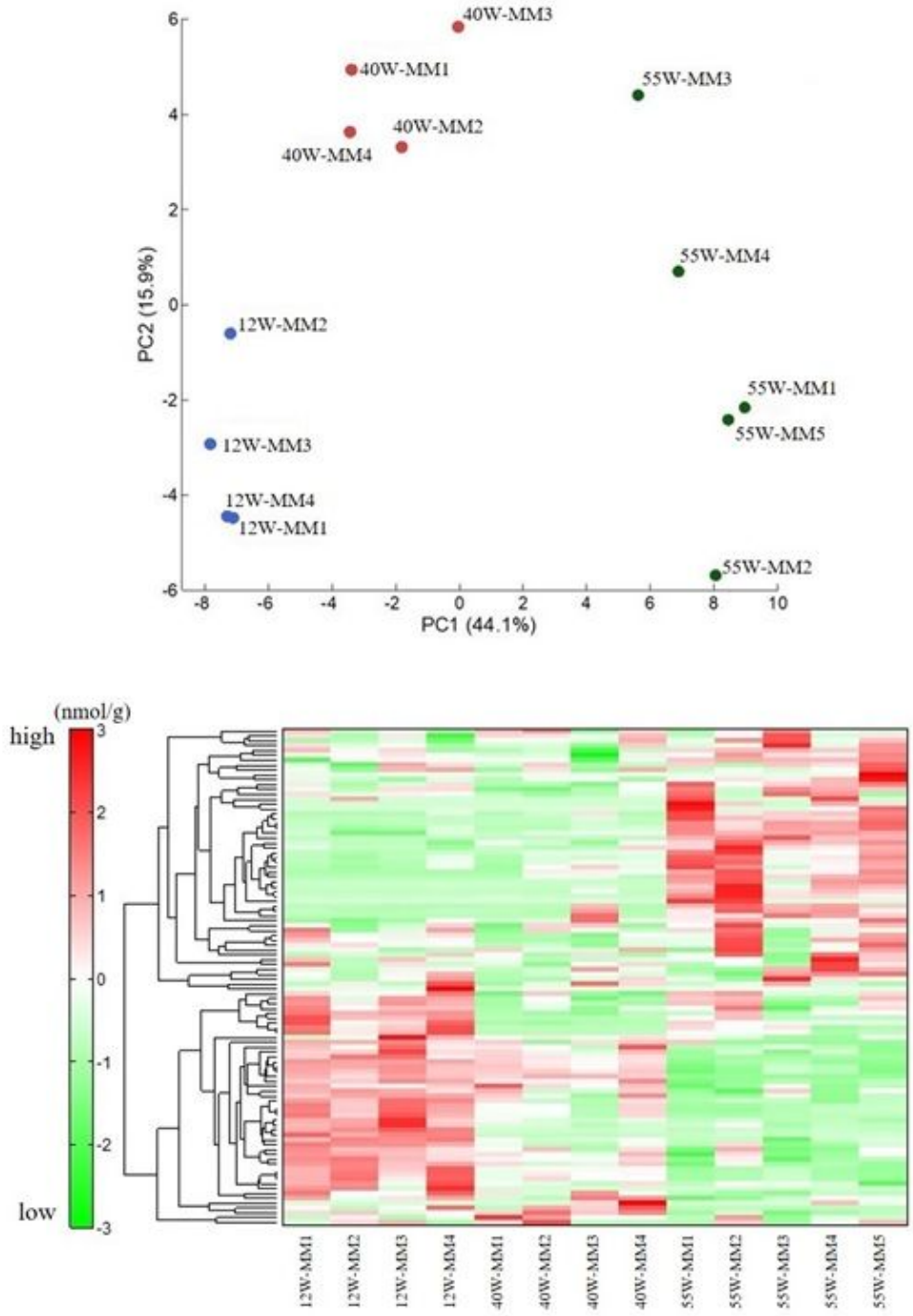

Figure 2

a Principal component analysis (PCA) of metabolomic datasets Principal component analysis (PCA) of metabolomic datasets of MM from 12-week-old and 40-week-old, 55-week-old. Plots of 12-week-old (blue circles) and 40-week-old (red circles), 55-week-old (green circles) mice are clearly distinguished on the first principal component axis (x-axis). b Hierarchical Cluster Analysis (HCA) of comparing metabolite changes among 12-week-old and 40-week-old, 55-week-old. The vertical axis shows sample names

corresponding to the samples used in Fig. 3 (12W-MM1 to 12W-MM4 for 12-week-old and 40W-MM1 to 40W-MM4 for 40-week-old, 55W-MM1 to 55W-MM5 for 55-week-old). Red indicates that the relative content of metabolites is high, whereas green indicates that the relative content of metabolites is low.

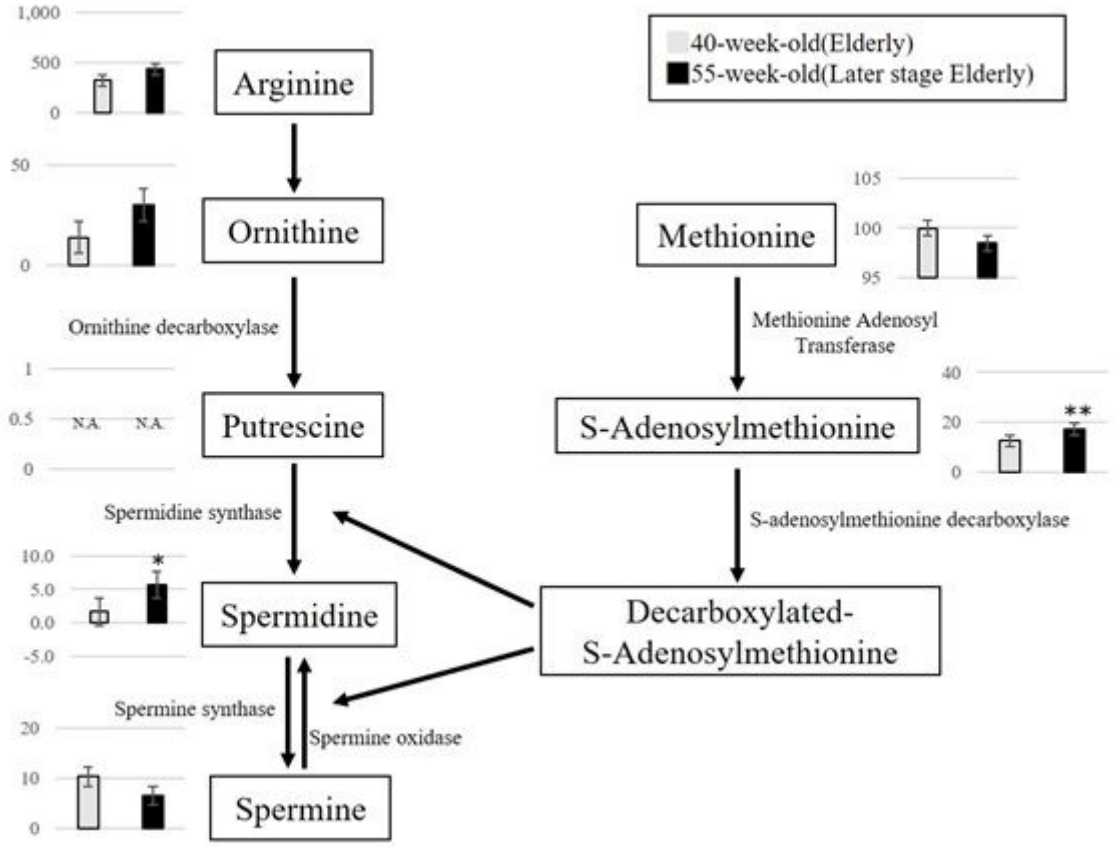

Figure 3

Pathway Map of Polyamine Metabolism Metabolic changes related to polyamine metabolism. (** $p < 0.01$, * $p < 0.05$)

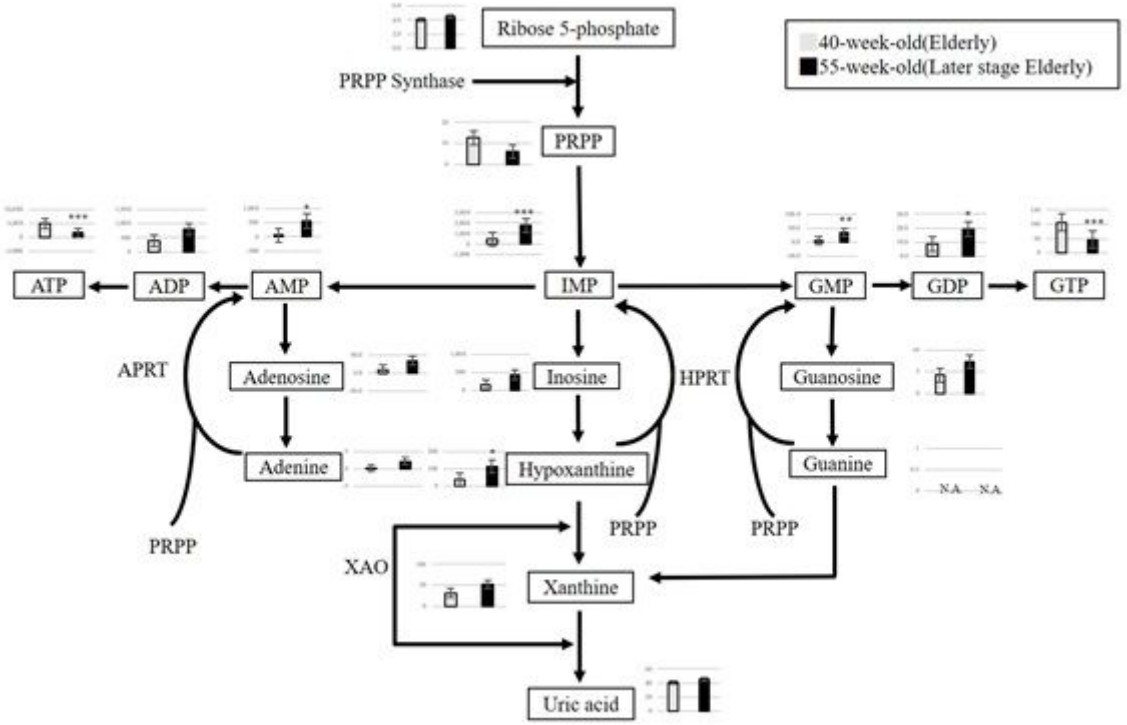

Figure 4

Pathway Map of Purine metabolism Metabolic changes related to purine metabolism. (***p < 0.001, ** p < 0.01, * p < 0.05)

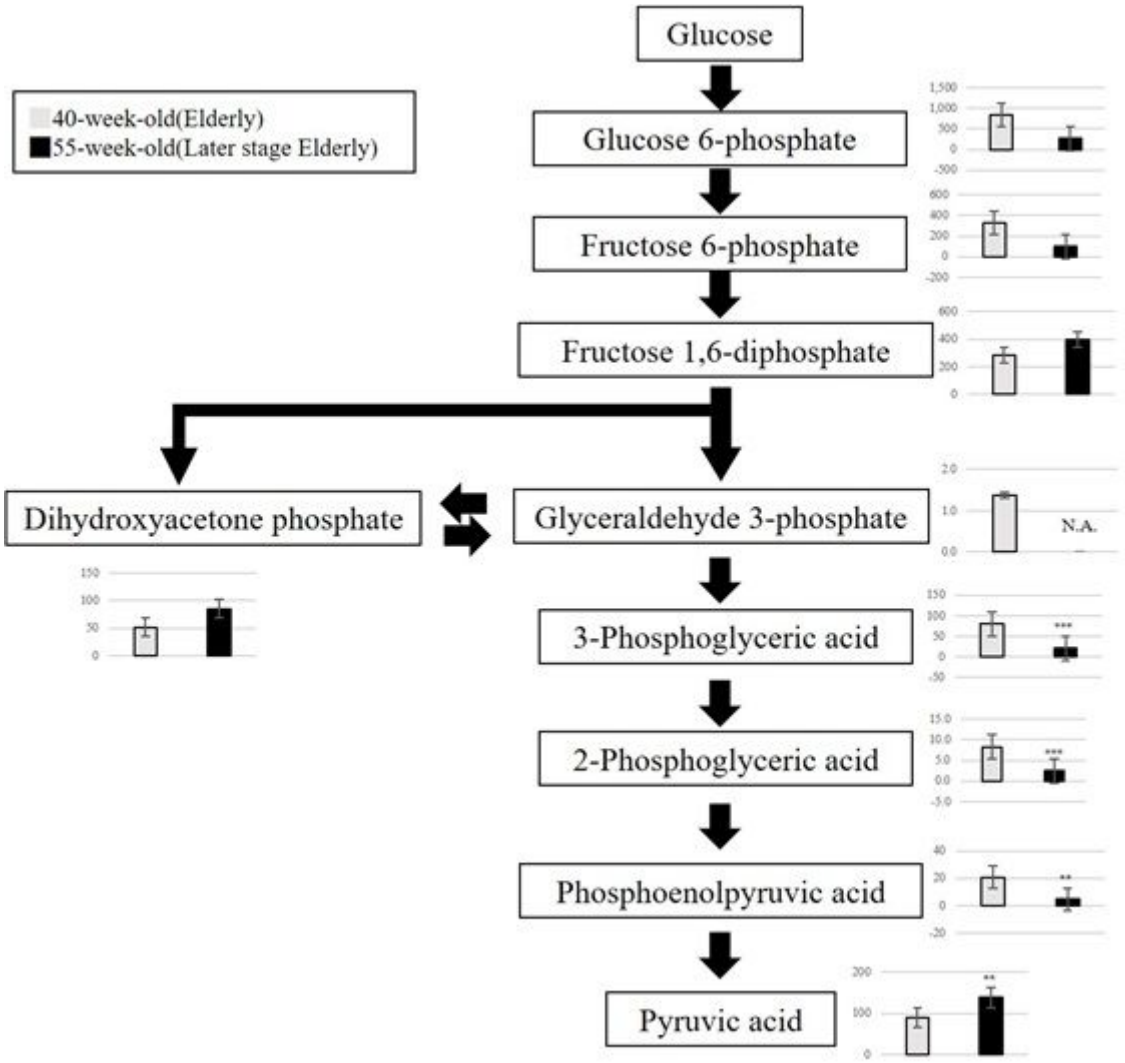

Figure 5

Pathway Map of Glycosis Metabolic changes related to polyamine metabolism. (*** $p < 0.001$, ** $p < 0.01$)

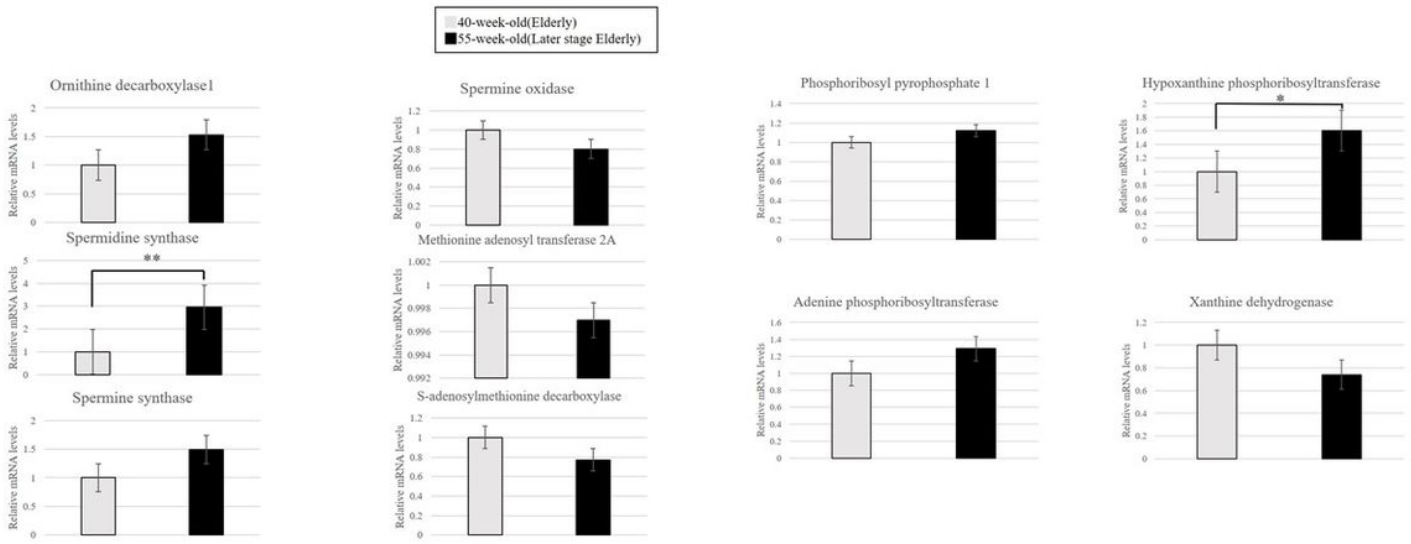

Figure 6

a RT-PCR of Polyamine Metabolism Gene expression of polyamine metabolism from 40-week-old and 55-week-old. Gray bars : 40-week-old, black bars : 55-week-old. (**p < 0.01). b RT-PCR of Purine Metabolism Gene expression of purine metabolism from 40-week-old and 55-week-old. Gray bars : elderly mice, black bars : later stage elderly mice. (*p < 0.05).

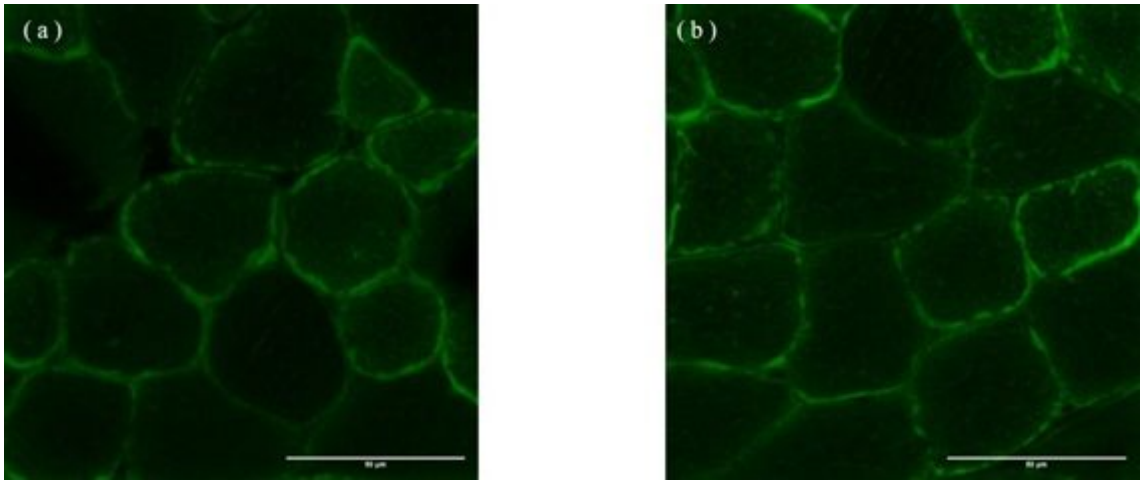

Figure 7

Immunohistochemical observation of SRM in cross-sectional area Immunohistochemically stained images acquired using SRM antibodies at each age are showed. SRM is green. (a) : 40-week-old, (b) : 55-week-old. Scale bar: 50 μm.

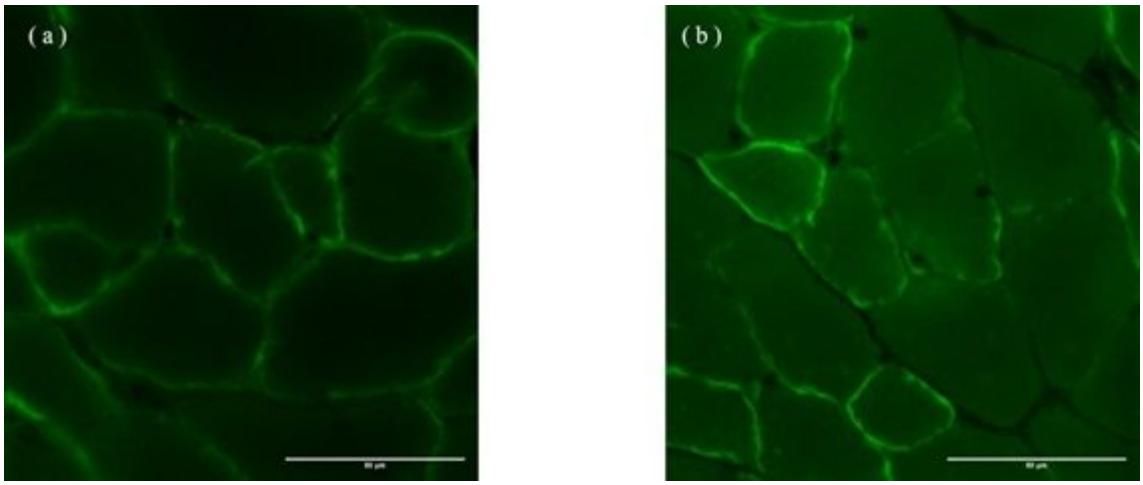

Figure 8

Immunohistochemical observation of HPRT in cross-sectional area Immunohistochemically stained images acquired using HPRT antibodies at each age are showed. HPRT is green. (a) : 40-week-old, (b) : 55-week-old. Scale bar: 50 μm.